Proceedings of the
2002 Fluids Engineering Division Summer Meeting
July 14 - 18, 2002, Montreal, Quebec, Canada

FEDSM2002-31418

STOCHASTIC ESTIMATION AND NON-LINEAR WALL-PRESSURE SOURCES IN A SEPARATING/REATTACHING FLOW

A. Naguib/Michigan State University **L. Hudy**/Michigan State University

W.M. Humphreys, Jr./NASA Langley Research Center

ABSTRACT

Simultaneous wall-pressure and PIV measurements are used to study the conditional flow field associated with surface-pressure generation in a separating/reattaching flow established over a fence-with-splitter-plate geometry. The conditional flow field is captured using linear and quadratic stochastic estimation based on the occurrence of positive and negative pressure events in the vicinity of the mean reattachment location. The results shed light on the dominant flow structures associated with significant wall-pressure generation. Furthermore, analysis based on the individual terms in the stochastic estimation expansion shows that both the linear and non-linear flow sources of the coherent (conditional) velocity field are equally important contributors to the generation of the conditional surface pressure.

INTRODUCTION

Understanding the flow generation mechanisms of wall-pressure fluctuations is important in engineering applications involving flow-induced noise/vibration and flow-structure interaction. It is well known that the dependence of the wall-pressure on the flow field is given through the solution of Poisson's equation that governs the pressure fluctuations for incompressible turbulent flows. This solution gives rise to two flow pressure sources: the first is known as the fast, or *linear*, pressure source and the second is the slow, or *non-linear* term.

Recently, Naguib *et al.* (2001) utilized stochastic estimation to study the conditional velocity field associated with single-point wall-pressure events in a turbulent boundary layer. It was found that for an accurate representation of the conditional velocity field, a quadratic, rather than linear, stochastic estimation must be used. More significantly, the following equations linking the conditional wall-pressure ($<p'_w>$) generated by the coherent (conditional) flow field to the different terms in the stochastic estimation were derived:

$$\frac{<p'_w>(x_o,z_o)}{\rho/2\pi} = \iiint 2\frac{\frac{dU}{dy}\frac{d<u'_2>_l}{dx}}{\sqrt{(x_o-x_s)^2+y_s^2+(z_o-z_s)^2}}dV_s \qquad [1]$$

$$\iiint \frac{\frac{\partial^2}{\partial x_i \partial x_j}<u'_i><u'_j>}{\sqrt{(x_o-x_s)^2+y_s^2+(z_o-z_s)^2}}dV_s = \iiint 2\frac{\frac{dU}{dy}\frac{d<u'_2>_q}{dx}}{\sqrt{(x_o-x_s)^2+y_s^2+(z_o-z_s)^2}}dV_s \qquad [2]$$

where x,y and z are the spatial coordinates in the streamwise, wall-normal and spanwise directions, respectively, U is the mean streamwise velocity and u'_i is the turbulent velocity (note that throughout this paper, tensor notation is used whenever convenient). The left-hand side of equations [1] and [2] represent the conditional wall pressure and the portion of it that is generated by the coherent non-linear sources, respectively. On the right hand side, the conditional flow sources reduce to the linear ($<u'_2>_l$) and quadratic ($<u'_2>_q$) components of the stochastic estimation of the *wall-normal* component of the turbulent velocity field.

Equations [1] and [2] are quite interesting in the sense that they show the following: 1) Knowledge of the linear term in a stochastic estimation of the wall-normal velocity component is sufficient to calculate the wall pressure generated by the conditional flow field at a point; 2) The quadratic term in the stochastic estimation is non-zero if the non-linear source mechanism contributes to the generation of the conditional pressure. This can be seen from equation [2] where vanishing of $<u'_2>_q$ results in zero non-linear wall pressure generation by the conditional velocity field; 3) Knowledge of the quadratic

component of the stochastic estimation of u'_2, instead of the full conditional Reynolds-stress-gradient, is sufficient to calculate the non-linear source contribution. It should be added here that equations [1] and [2] pertain to flows that are two-dimensional in the mean and assume that a quadratic, and not a higher-order, stochastic estimation converges to the conditional velocity field satisfactorily.

NOMENCLATURE

$A_{i,lin}$: Linear Coefficient of LSE of Velocity u'_i
$A_{i,quad}$: Linear Coefficient of QSE of Velocity u'_i
B_i : Quadratic Coefficient of QSE of Velocity u'_i
h_f : Fence Height Above Splitter Plate
LSE : Linear Stochastic Estimation
p'_w : Turbulent Wall Pressure
QSE : Quadratic Stochastic Estimation
$\vec{r}_o$: Wall-Pressure Event Location
rms : Root Mean Square
U : Mean Streamwise Velocity
U_o : Free-Stream Velocity
u'_i : Turbulent Velocity Vector
$\tilde{u}'_i$: Stochastically Estimated Velocity Vector
$< u'_i >_l$: Linear Component of $\tilde{u}'_i$
$< u'_i >_q$: Quadratic Component of $\tilde{u}'_i$
x,y,z : Spatial Coordinates
x_r : Mean Reattachment Length
τ : Time Offset
$\Delta \vec{r}$: Spatial Offset
$< >$: Conditional Average

OBJECTIVES

In this paper, the analysis of Naguib *et al.* (2001) is extended to a newly acquired database of simultaneous Particle Image Velocimetery (PIV) and wall-microphone array measurements in a separating/reattaching flow configuration. The primary objectives of the paper are to (1) study the conditional flow features associated with wall-pressure generation in the vicinity of the mean reattachment position (x_r), and (2) examine the relative importance of the corresponding linear and non-linear flow sources.

It is worthwhile to note here that the current paper has focused on using the stochastic estimation analysis based on single-point events because of the usefulness of this approach in analyzing the relative importance of the linear and non-linear p'_w sources of the conditional velocity field. However, evidence that Linear Stochastic Estimation (LSE) coupled with multi-point event could provide a better estimation of the dominant flow structure than single-point LSE may be found in the work of Bonnet *et al.* (1998), amongst others. Thus, if one's main concern is to obtain the most efficient model of the flow, multi-point estimation is generally more appropriate.

EXPERIMENT

The experiment used to compile the data set for this study was conducted in the Subsonic Basic Research Tunnel (SBRT) at NASA Langley Research Center in Hampton, Virginia. The dimensions of the test section were 0.57 m × 0.82 m × 1.85 m in width, height and length, respectively. A model consisting of a splitter plate downstream of a fence was placed horizontally at the center of the test section to generate a separating/reattaching flow. Figure 1 provides a schematic of the model side view and associated coordinate system. Also included in the figure are the mean-flow streamlines and the location of the focus area of the current PIV measurements. The streamlines were obtained from the study of Castro and Haque (1987) of a flow geometry identical to the current one. In fact, the coefficient of mean-wall-pressure distribution along the model centerline from this study agrees very well with that from Castro and Haque (Hudy *et al.*, 2002). Also note that although the streamlines in Figure 1 have been drawn to scale, the vertical dimension was stretched relative to the horizontal one in order to make the flow pattern visible. Moreover, the dashed lines identify the edges of the separating shear layer (also based on Castro and Haque's measurements).

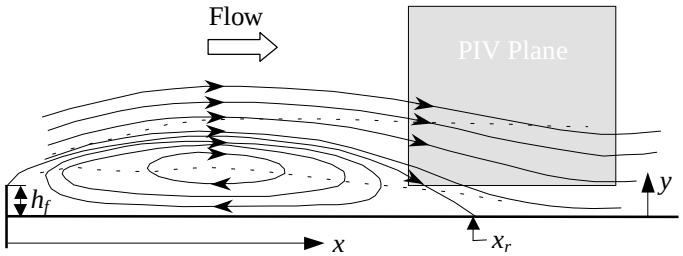

Figure 1. Test Model Schematic (Steamlines after Castro and Haque, 1987)

For the experiments discussed here, the flow speed upstream of the model (U_o) was set to 15 m/s, resulting in a Reynolds number of approximately 8000 (based on the fence height above the splitter plate, h_f). The corresponding freestream turbulence intensity was less than 3%. PIV measurements were conducted over a plane parallel to the streamwise (x) and normal (y) directions and centered on top of a 28 wall-microphone array along the centerline of the model. Details of the test model and the wall-pressure and PIV measurements may be found in Hudy *et al.* (2002) and Humphreys and Bartram (2001).

The PIV measurements yielded a total of 35×18 velocity vectors in the streamwise and normal directions, respectively, at a spacing of 2.5 mm. False vectors introduced by the cross-correlation analyses were identified via magnitude comparison and discarded. The remaining vector field was smoothed using a 3×3 Gaussian window, producing velocity vectors in a region extending approximately from $0.8x_r$ to $1.3x_r$ in the

streamwise direction, and from h_f to $6h_f$ in the y direction. For $y < h_f$, the seeding density was generally insufficient to provide accurate vectors. Notwithstanding this limitation, the bulk of the separated shear layer is resolved with the current measurements, allowing examination of the shear-layer flow sources of the wall pressure. It is generally believed that these sources, or structures, dominate the surface-pressure generation process in the vicinity of the mean reattachment point; e.g., see Cherry *et al.* (1984).

The mean velocity vector field and associated streamlines obtained from the current data are shown in Figure 2. The coordinates of the vector plot have been normalized using x_r, which was estimated from the mean wall-pressure data (see Hudy *et al.* (2002) for details). Also, the fence height is provided in the figure for reference. The observed characteristics of the vector field in Figure 2 are consistent with the expected behavior of the test flow in the PIV field of view delineated in Figure 1.

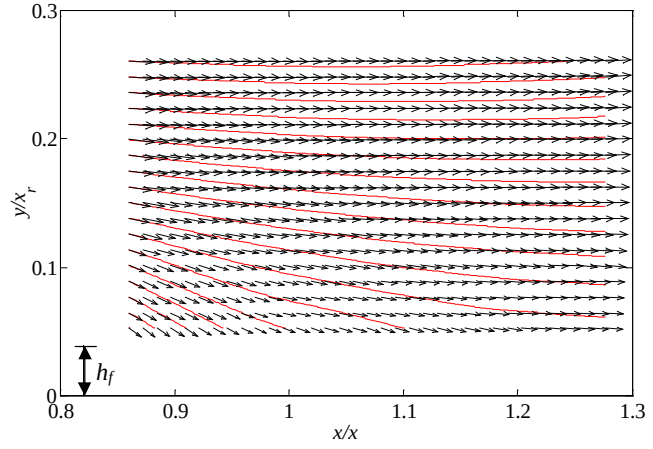

Figure 2. Mean-Velocity Vector Field and Streamlines

STOCHASTIC ESTIMATION

As outlined in the objectives, stochastic estimation is used here as a tool to estimate the turbulent velocity field above the wall, $u'_i(\vec{r}_o + \Delta\vec{r}, t+\tau)$, from a known wall-pressure magnitude, or event, $p'_w(\vec{r}_o, t)$; where $\vec{r}_o = (x_o, 0, z_o)$ is the location of the event, $\Delta\vec{r} = (x - x_o, y, z - z_o)$ is the offset between the estimate and event locations, and τ is the corresponding time offset. The stochastically estimated velocity field, $\tilde{u}'_i(\vec{r}_o + \Delta\vec{r}, t+\tau)$, is obtained from a Taylor series expansion of the estimate in terms of the known condition (the wall pressure in the current work). The series expansion converges to the conditionally averaged velocity field: $< u'_i(\vec{r}_o + \Delta\vec{r}, t+\tau) >$. If the linear term alone represents the conditional field accurately, the estimate is known as Linear Stochastic Estimation, or LSE. On the other hand, if the second order term in the series is included in the estimation, a Quadratic Stochastic Estimation (QSE) is obtained. See Naguib *et al.* (2001) for a comprehensive list of literature on stochastic estimation.

The LSE equation for the velocity field in terms of the wall-pressure event is given by:

$$\tilde{u}'_i(\vec{r}_o + \Delta\vec{r}, t+\tau) = A_{i,\mathrm{lin}}(\Delta\vec{r}, \tau; \vec{r}_o)\, p'_w(\vec{r}_o, t) \qquad [3]$$

and,

$$A_{i,\mathrm{lin}}(\Delta\vec{r}, \tau; \vec{r}_o) = \frac{R_{p'u'_i}(\Delta\vec{r}, \tau; \vec{r}_o)}{p'^2_{w,rms}(\vec{r}_o)} \qquad [4]$$

where $R_{p'u'_i}$ is the correlation function between p'_w and u'_i, and subscript *rms* denotes the root-mean-square value. Note that the linear coefficient in LSE, $A_{i,\mathrm{lin}}$, is taken to be a function of the temporal separation between the event and estimate, but not the specific time where the event is observed. This is permissible because the flow is stationary. The same is not true for the space variable because of the non-homogeneous character of the flow in the streamwise direction. On the other hand, the QSE equation has the form:

$$\tilde{u}'_i(\vec{r}_o + \Delta\vec{r}, t+\tau) = A_{i,\mathrm{quad}}(\Delta\vec{r}, \tau; \vec{r}_o)\, p'_w(\vec{r}_o, t) + B_i(\Delta\vec{r}, \tau; \vec{r}_o)\, p'^2_w(\vec{r}_o, t) \qquad [5]$$

$$A_{i,\mathrm{quad}}(\Delta\vec{r}, \tau; \vec{r}_o) = A_{i,\mathrm{lin}}(\Delta\vec{r}, \tau; \vec{r}_o) - B_i(\Delta\vec{r}, \tau; r_o)\frac{\overline{p'^3_w(\vec{r}_o)}}{p'^2_{w,rms}(\vec{r}_o)} \qquad [6]$$

$$B_i(\Delta\vec{r}, \tau; \vec{r}_o) = \frac{\overline{p'^3_w(\vec{r}_o)}R_{p'u'_i}(\Delta\vec{r}, \tau; \vec{r}_o) - p'^2_{w,rms}(\vec{r}_o)R_{p'p'u'_i}(\Delta\vec{r}, \tau; \vec{r}_o)}{p'^2_{w,rms}(\vec{r}_o)\overline{p'^4_w(\vec{r}_o)} - \left[\overline{p'^3_w(\vec{r}_o)}\right]^2} \qquad [7]$$

where, $R_{p'p'u'_i}$ is the correlation function between p'^2_w and u'_i and the over-bar denotes time averaging. It is interesting to note that the form of the linear term coefficient in the stochastic estimation is different for the linear, $A_{i,\mathrm{lin}}$, and quadratic, $A_{i,\mathrm{quad}}$, estimates. Equations [3] through [7] show that in order to compute LSE and QSE coefficients, one needs to compute the two-point space-time correlation functions $R_{p'u'_i}$ and $R_{p'p'u'_i}$ as well as the second-, third- and fourth-order moments of the probability density function of the wall pressure at the location of the event. In this paper, the velocity field is only estimated at the time of occurrence of the event (i.e., $\tau = 0$) for pressure events occurring at $x/x_r = 0.97$ (i.e., $\vec{r}_o = (0.97x_r, 0, 0)$; where $z = 0$ is on the centerline of the test model).

The LSE vector fields associated with positive and negative wall-pressure events of magnitude $2p'_{w,rms}$ may be seen in the top and bottom portions, respectively, of Figure 3. Note that all velocity vector fields are presented here as viewed

in a frame of reference with a *streamwise* translation velocity of $0.53U_o$, which is equal to the convection velocity of the dominant wall-pressure signature. This velocity was estimated from the wall-microphone-array data using the phase characteristics of the pressure fluctuations at a frequency corresponding to the wall-pressure spectrum peak at x_r. Details of the estimation procedure may be found in Hudy (2001).

In both vector plots shown in Figure 3, a flow pattern with substantial streamwise variation in u'_2 is found at the lowest y position, on top and slightly upstream of the location of the pressure event. This near-wall *localized* shear-layer-like flow is reminiscent of the conditional velocity obtained in the buffer region of a turbulent boundary layer for positive and negative wall-pressure occurrences (e.g., Johansson *et al*., 1987). The positive pressure event is associated with 'in-rushing' fluid towards the wall, whereas in the case of the negative event, fluid is seen moving away from the wall.

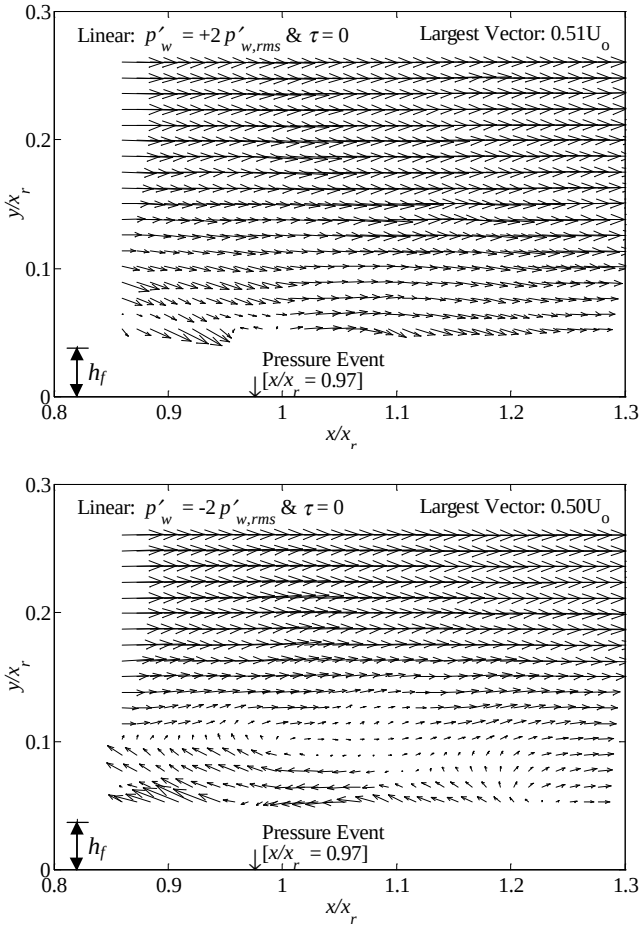

Figure 3. LSE Vector Fields for Positive (top) and Negative (bottom) Wall-Pressure Events at x/x_r = 0.97

The QSE vector fields are shown in Figure 4 for the same wall-pressure condition used for the LSE results. Although the general features of the LSE and QSE vector fields are similar, some important differences are observed for the case of negative condition. First, a vortical motion (the center of which is marked by × on the bottom plot of Figure 4) is now observed above the reattachment point. This appears to be consistent with the general belief that negative wall-pressure occurrences in separated/reattaching flows is associated with passage of the low-pressure cores of the separated-shear-layer vortical structures. To further verify this viewpoint, the wall-normal mean-velocity profile and its gradient at x_r are shown in Figure 5 along with the y location of the observed vortex center. It is evident from these results that the center of the vortex is located very close to the inflection point (maximum velocity gradient) of the mean velocity profile, which is at the center of the reattaching shear layer.

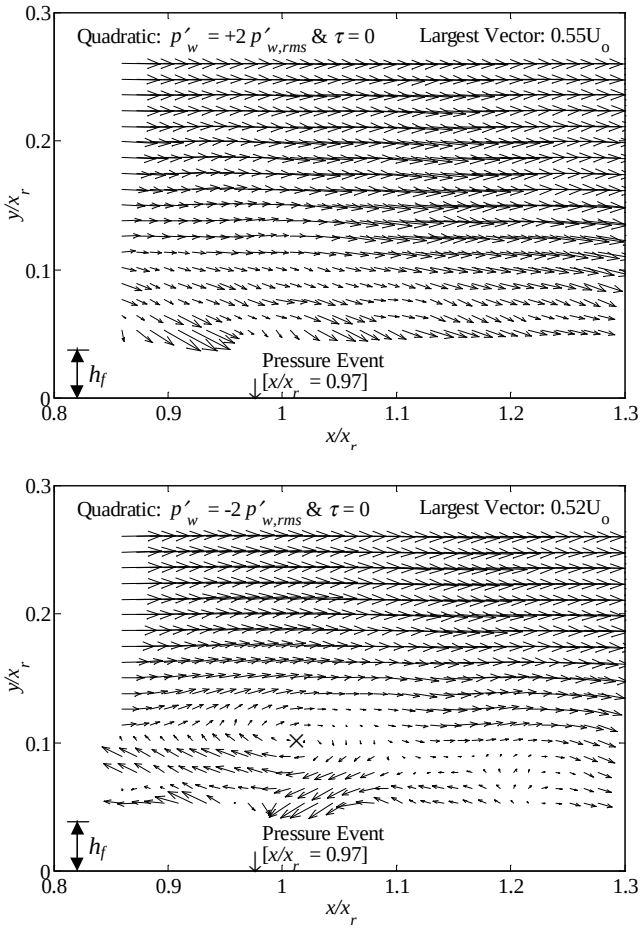

Figure 4. QSE Vector Fields for Positive (top) and Negative (bottom) Wall-Pressure Events at x/x_r = 0.97

In addition to the vortex structure, QSE results for negative pressure reveal a new region of substantial streamwise variation in the normal velocity above and immediately downstream of x_r. This streamwise variation in the quadratic component of u'_2, which is depicted at the lowest

y position and roughly in the range x/x_r = 0.95 – 1.08, is likely to give rise to non-linear wall-pressure generation, as discussed in the introduction.

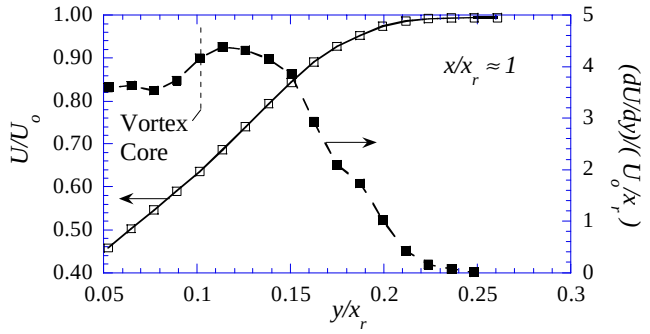

Figure 5. Mean Velocity and Velocity-Gradient Profiles at $x/x_r \approx 1$

Equations [1] and [2] show that in addition to the mean streamwise velocity field, only the linear and quadratic QSE components of u'^2 are required in order to calculate the source function (integrand) for the *total* and *non-linear*, respectively, generation of the conditional pressure. Hence, the strength of these sources was calculated by evaluating the derivatives in equations [1] and [2] using a finite difference scheme. Subsequently, the strength of the *linear* source was calculated by subtracting the non-linear component from the total contribution. It should be noted that equations [1] and [2] are built on the assumption that dU/dy is the only mean-strain component. In the flow considered here, other mean-strain components are non-zero. However, near the centerline of the model, dU/dy is the most dominant shear component, particularly near the wall. Therefore, only dU/dy is considered in this paper.

Figure 6 displays the strength of the linear, non-linear and total sources of the conditional wall pressure at x/x_r = 0.97 for a positive pressure event at two heights: y/x_r = 0.052 (bottom plot) and 0.064 (top plot). Similar plots for a negative event are provided in Figure 7. Note that the source strength results have been made non-dimensional using U_o and x_r. Also, results at higher y positions are not included in the figure since they depict weaker source strength than that found at y = 0.064. Moreover, it should be pointed out that although it has not been investigated whether cubic and higher order terms are also important in the stochastic estimation, it can be shown that their elimination results in underestimation of the non-linear source strength. For the turbulent boundary layer of Naguib *et al*. (2001), a quadratic expansion yielded accurate representation of the conditional velocity field.

Consideration of Figures 6 and 7 shows that the most intense sources of the conditional wall-pressure, regardless of sign, are located at the lowest y position and above/immediately-upstream of the event location. This is the same region in the flow where the near-wall shear-layer has been depicted in the LSE results.

Of particular interest is the fact that in the negative wall-pressure case, the reattaching-shear-layer vortex structure captured in the QSE velocity field above x_r is a substantially less important source of wall pressure fluctuations than the localized near-wall shear layer. This is a significant conclusion since traditionally negative wall-pressure peaks in separating/reattaching flows have been assumed to be caused by the low-pressure cores of the separating shear-layer vortical structures. The analysis done here suggests that although the association of the negative pressure peaks with these vortical structures seem to be true, the suction wall-pressure seems to be generated by near-wall localized shear layers rather than by the low-pressure cores of these structures. It may be the case that as the vortices travel downstream, they induce/initiate the formation of the near-wall shear layers (perhaps through interaction with the wall or other vortical structures). Additional investigation is required to elaborate further on this issue.

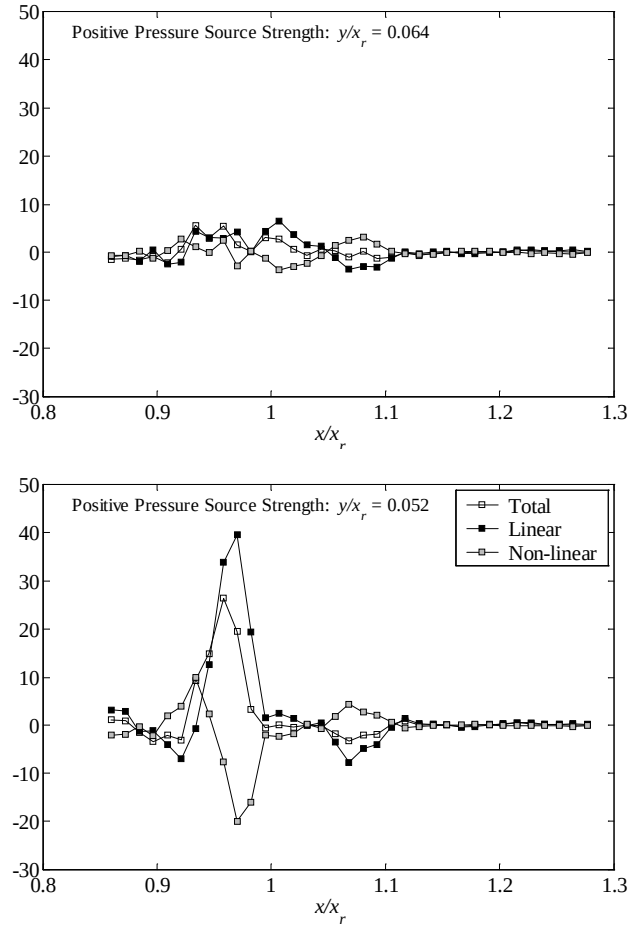

Figure 6. Coherent Flow Sources of Positive Conditional Wall-Pressure at x/x_r = 0.97 and y/x_r = 0.052 (bottom) & 0.062 (top)

Another interesting aspect of the results in Figures 6 and 7 is that they indicate that the contributions of both the linear

and non-linear sources to the wall-pressure generation are equally important. This is deduced form the similar order of magnitude of these sources for both positive and negative events. For the former, the most intense linear and non-linear sources appear to occupy the same location. This is unlike the negative-pressure event sources, where the strongest linear source appears to be located upstream of the strongest non-linear source of negative wall-pressure. Finally, it should be noted that because of its even power dependence on the pressure event, the non-linear source contribution is independent of the sign of the pressure event.

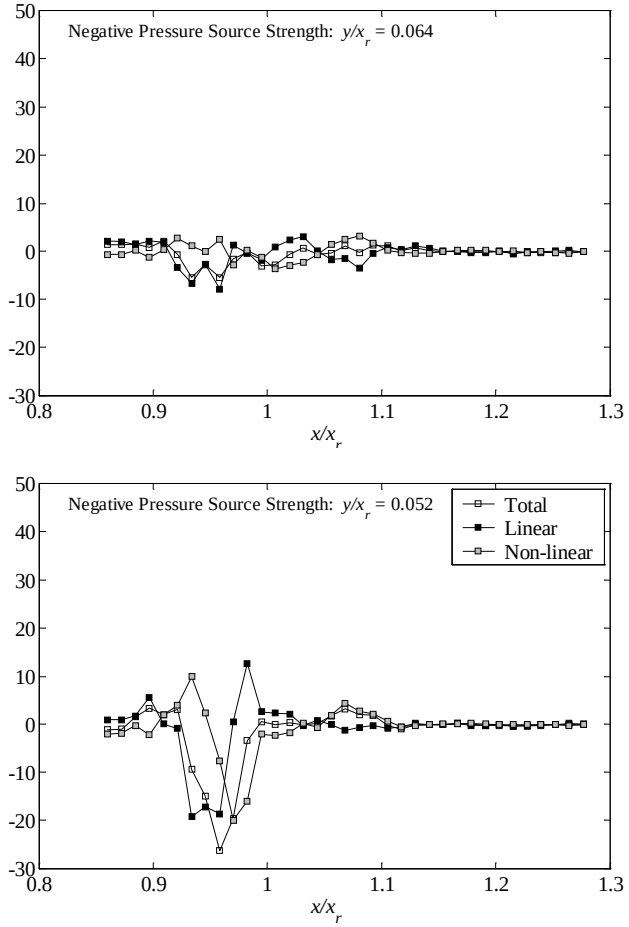

Figure 7. Coherent Flow Sources of Negative Conditional Wall-Pressure at x/x_r = 0.97 and y/x_r = 0.052 (bottom) & 0.062 (top)

SUMMARY

Stochastic Estimation is used to examine the flow structure associated with significant wall-pressure generation in the vicinity of the reattachment point of the flow over a fence with a splitter plate in its wake. The results show that linear stochastic estimation provides good qualitative description of the flow structure associated with positive wall-pressure events. However, for negative events, inclusion of the quadratic term shows a clear association with vortical motion in the reattaching shear layer, which is not captured in the linear estimation. Furthermore, analysis of the coherent sources of the wall-pressure using the linear and quadratic terms suggests that the negative wall pressure is generated by localized energetic near-wall shear layers, rather than by the low-pressure core of the vortex structures. Moreover, both linear and non-linear flow sources of the wall pressure are found to be equally important.

ACKNOWLEDGMENTS

The authors would like to acknowledge the support of the Advanced Measurement and Diagnostics Branch at NASA Langley Research Center of this work, including the support of L. Hudy under a GSRP grant. Also, this work would not be possible without the hard work of Scott M. Bartram in setting up and ensuring the quality of the data obtained from the PIV and wall-pressure measurements.

REFERENCES

J.P. Bonnet, J. Delville, M.N. Glauser, R.A. Antonia, D.K. Bisset, D.R. Cole, H.E. Fiedler, J.H. Garem, D. Hilberg, J. Jeong, N.K.R. Kevlahan, L.S. Ukeiley and E. Vincendeau, "Collaborative Testing of Eddy Structure Identification Methods in Free Turbulent Shear Flows," Exp. Fluids, **25**, 197 (1998).

I.P. Castro and A. Haque, "The Structure of a Turbulent Shear Layer Bounding a Separation Region," J. Fluid Mech., **179**, 439 (1987).

N.J. Cherry, R. Hillier and M.E.M.P. Latour, "Unsteady Measurements in a Separated and Reattaching Flow," J. Fluid Mech., **144**, 13 (1984).

L. Hudy, "Simultaneous Wall-Pressure Array and PIV Measurements in a Separating/Reattaching Flow Region," Master Thesis, Michigan State University (2001).

L. Hudy, A. Naguib, W.M. Humphreys, Jr. and S.M. Bartram, "Wall-Pressure Measurements Beneath a Separating/Reattaching Flow Region," AIAA Paper No. 2002-0579, 40th AIAA Aerospace Sciences Meeting & Exhibit, Reno, Nevada, January 14-17 (2002).

W.M. Humphreys, Jr. and S.M. Bartram, "Measurement of Separated Flow Structures Using a Multiple-Camera DPIV System", 19th ICIASF Conference, Cleveland, Ohio, August 27-30 (2001).

A. V. Johansson, J. Y. Her and J. H. Haritonidis, "On the Generation of High-Amplitude Wall-Pressure Peaks in Turbulent Boundary Layers and Spots," J. Fluid Mech., **175**,119 (1987).

A. Naguib, C. Wark and O. Juckenhoefel, "Stochastic Estimation and Flow Sources Associated with Surface Pressure Events in a Turbulent Boundary Layer," Physics of Fluids, **13**, No. 9, 2611 (2001).